JMEPEG
https://doi.org/10.1007/s11665-024-10077-6

1059-9495/$19.00

ORIGINAL RESEARCH ARTICLE

Combined Effect of Annealing Temperature and Pre-deformation on the Superelastic Behaviors of NiTi Shape Memory Alloys

Xiangguang Kong, Jiaqi Zhang, Haimin Ding, Qing Liu, Jiyu Zhou, Fugong Qi, and Pengjie Wang

Submitted: 28 June 2024 / Revised: 28 July 2024 / Accepted: 9 August 2024

The combined effect of annealing temperature and pre-deformation on the superelastic behaviors of NiTi shape memory alloy wires was investigated by testing two types of samples with 72 and 35% area reduction. It is found that the annealed samples with 72% area reduction exhibited larger martensitic transformation stress, and the annealed samples with 35% area reduction exhibited superior superelastic cycle stability. The stress hysteresis of martensitic transformation for both two types of samples decreased with decreasing annealing temperature. In addition, pre-deformation enhanced the superelastic cycle stability and increased the stress hysteresis of the NiTi wires with 72% area reduction, but it had little effect on the stress hysteresis of the NiTi wires with 35% area reduction.

Keywords annealing, NiTi, shape memory alloy, stress hysteresis, superelastic

1. Introduction

NiTi shape memory alloys (SMAs) have attracted considerable attention due to their unique functional properties, including shape memory effect and superelasticity (Ref 1-3). Among them, superelasticity arises from a reversible phase transformation between the austenite and martensite phases, which can be triggered by applied stress (Ref 4, 5). The critical stress of martensitic transformation, cyclic stability and stress hysteresis are the typical characteristics of the superelastic NiTi alloys. It is well reported that above characteristics are sensitive to the microstructure of NiTi alloys, such as grain size and dislocation (Ref 6-11).

The microstructure of NiTi alloys is directly affected by the machining and annealing process, such as the amount of machining deformation and annealing temperature (Ref 7, 8, 12-14). Recent works have found that the superelastic behaviors of NiTi alloys are not only affected by the annealing temperature, but also the amount of machining deformation. For example, Sun et al. observed a decrease in stress hysteresis with decreasing grain size in NiTi sheets produced through cold-rolling, which was attributed to the increased interfacial energy between the austenite and martensite phases (Ref 8). Differently, Shi et al. had found that the stress hysteresis of NiTi wires was affected by the amount of machining deformation, specifically, the stress hysteresis of samples with 75% area reduction increased with decreasing grain size, whereas that of samples with 39% area reduction decreased (Ref 7). Shi et al. attributed above behaviors to the difference between the grain size effect and the dislocation density effect on the stress hysteresis. However, R-phase in the annealed samples with 75% area reduction may play an important role for the increase in stress hysteresis (Ref 15, 16). Additionally, the effect of plastic deformation or pre-deformation on martensitic transformations differs significantly between the coarse-grained and nanocrystalline NiTi alloys (Ref 17-19). However, to our knowledge, no attempt has been undertaken so far to investigate the effect of plastic deformation on martensitic transformations of NiTi alloys with different amounts of machining deformation.

In this study, the combined effect of machining deformation, annealing temperature and pre-deformation on the superelastic behaviors of NiTi shape memory alloy wires was studied by transmission electron microscopy (TEM) observation and tensile testing. Our findings reveal the synergistic effect of grain size, dislocation and plastic deformation on the stress-induced martensitic transformation (SIMT) of NiTi wires.

2. Experimental Procedures

A commercial $Ni_{50.97}Ti_{49.03}$ (at.%) wire of 0.75 mm in diameter was obtained from JiYi Materials Co. Ltd. The wire of 0.62 mm in diameter was annealed at 750 °C for 180 s followed by air cooling and then cold drawn into diameters of 0.33 and 0.50 mm, effecting area reductions of approxi-

Xiangguang Kong and **Haimin Ding**, School of Energy, Power and Mechanical Engineering, North China Electric Power University, Baoding 071003, China; Hebei Key Laboratory of Electric Machinery Health Maintenance & Failure Prevention, North China Electric Power University, Baoding 071003, China; and Hebei Engineering Research Center for Advanced Manufacturing & Intelligent Operation and Maintenance of Electric Power Machinery, North China Electric Power University, Baoding 071003, China; and **Jiaqi Zhang, Qing Liu, Jiyu Zhou, Fugong Qi,** and **Pengjie Wang**, School of Energy, Power and Mechanical Engineering, North China Electric Power University, Baoding 071003, China. Contact e-mail: kongxiangguang@ncepu.edu.cn.

Published online: 12 September 2024

mately 72 and 35%, respectively. The samples having a length of 100 mm cut from the wires of 0.33 and 0.50 mm in diameter were annealed in air at 320, 360, 400 and 500 °C for 0.6 ks, respectively.

The microstructure of the samples was measured by transmission electron microscopy (TEM). Samples used for TEM observation were mechanically polished and finally ion milled using a Gatan 691 PIPS. The TEM observation was carried out using FEI Tecnai F20 and JEOL JEM 2100 (operating at 200 kV). Uniaxial tensile tests were performed on the NiTi wire samples at a strain rate of 5×10^{-4} s^{-1} using an Instron universal testing machine at to characterize the deformation behavior. The stress hysteresis was acquired by measuring the stress difference between the stresses of the 3% strain in the upper plateau and the 2.5% strain in the lower plateau during the 4% strain deformation cycle.

3. Results

3.1 Sample with 72% area Reduction

Figure 1 shows the TEM bright-field images and corresponding SAED patterns of the NiTi wires with 72% area reduction. Figure 1(a) shows the TEM bright-field image and corresponding SAED pattern of the unannealed sample. The SAED pattern shows significant broad diffuse rings corresponding to the amorphous phase. In addition, it can be seen that a small amount of nanograins with grain size less than 10 nm embedded in the amorphous NiTi matrix. The existence of these nanocrystals can provide non-uniform nucleation points for the crystallization of amorphous NiTi alloys, so that smaller-sized nanograins can be obtained after crystallization heat treatment. Figure 1(b) shows the TEM bright-field image and corresponding SAED pattern of the sample annealed at 320 °C. The TEM bright-field image shows a completely nanocrystalline structure, and the SAED pattern reveals no diffused ring, which indicates that the amorphous phase has been fully crystallized after annealing. The average grain size of this sample is about 20 nm based on the manual measurement of 200 grains. Figure 1(c) and (d) shows the TEM bright-field images and corresponding SAED patterns of the samples annealed at 400 and 500 °C, respectively. The average grain sizes of these two samples are approximately 23 and 85 nm, respectively.

Figure 2 shows the strain-controlled multi-step cyclic tensile curves (strains: 4%, 6% and 8%) of the annealed NiTi wires with 72% area reduction. It can be seen that all annealed samples exhibited flow stress upon loading and unloading, which demonstrated the occurrence of Lüders-type stress-induced martensitic transformation behavior (Ref 20). However, the Lüders plateau strain of 320 °C annealed sample is significantly lower than those of the other samples. In addition, it should be mentioned that in 320, 360 and 400 °C annealed

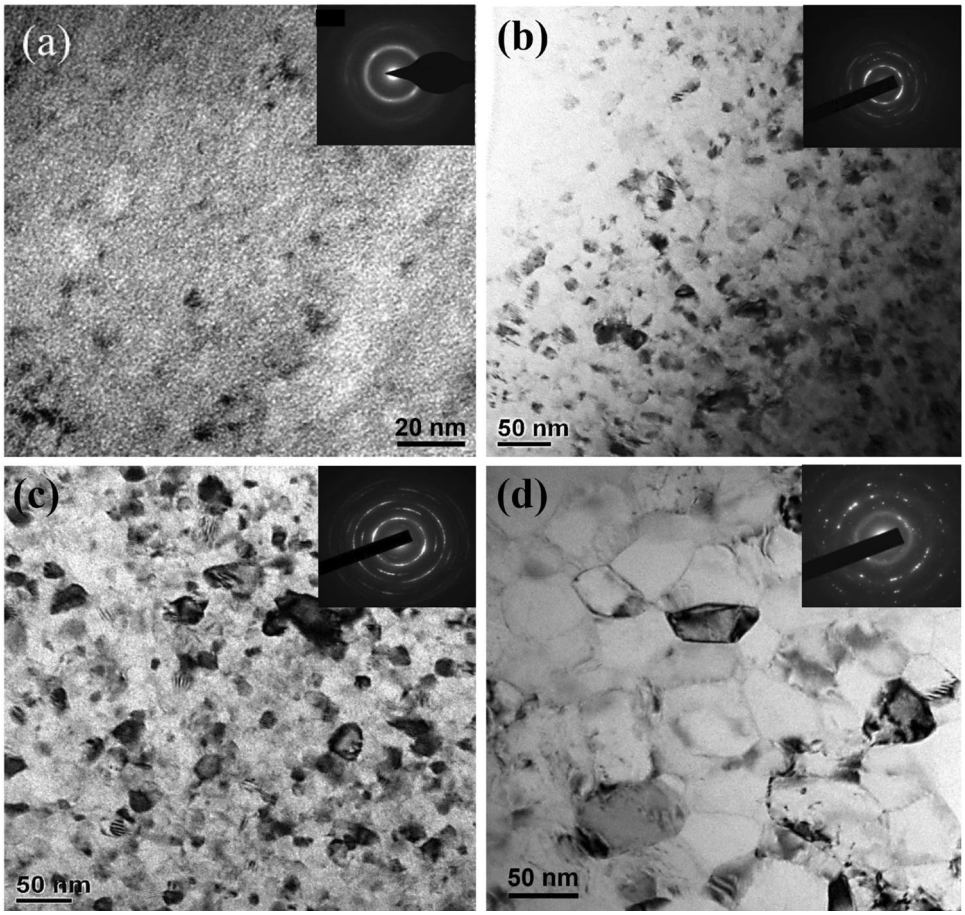

Fig. 1 TEM bright-field images and corresponding SAED patterns of the NiTi wires with 72% area reduction. (a) The unannealed sample; (b) the 320 °C annealed sample, (c) the 400 °C annealed sample; (d) the 500 °C annealed sample

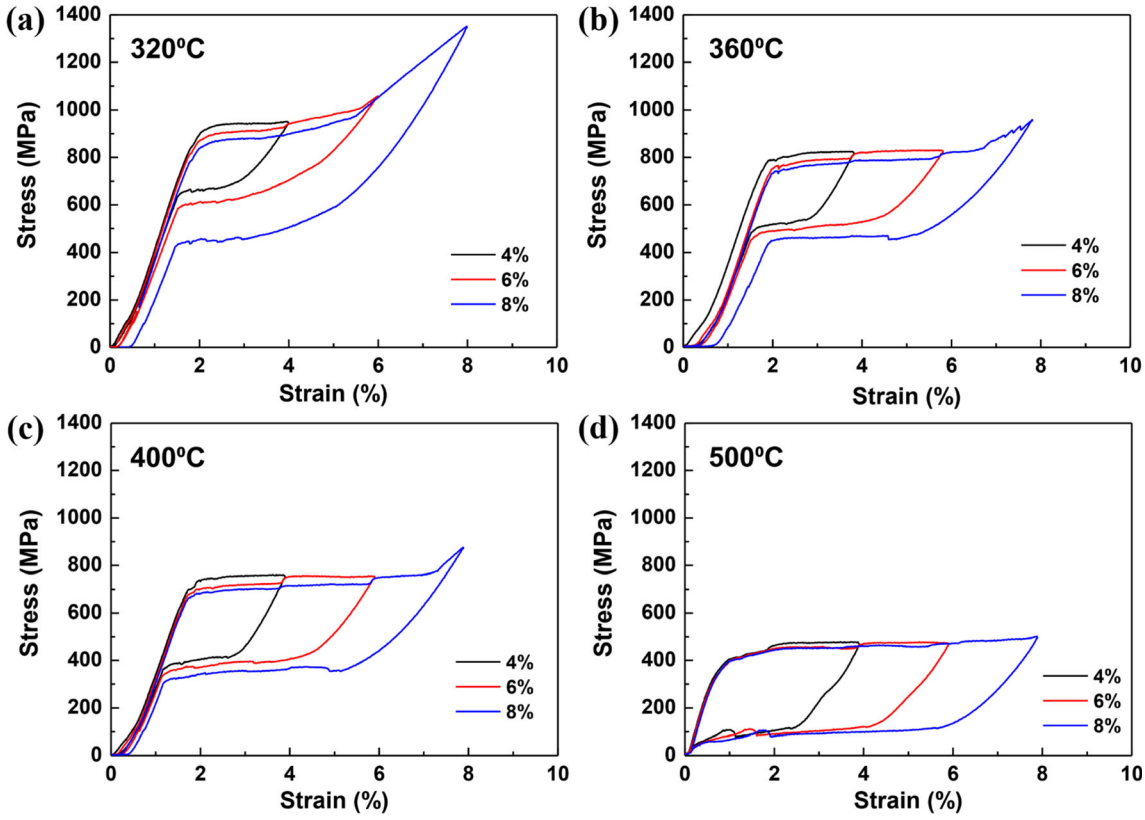

Fig. 2 Strain-controlled multi-step cyclic tensile curves (strains: 4%, 6% and 8%) of the annealed NiTi wires with 72% area reduction. (a) 320 °C annealed sample; (b) 360 °C annealed sample; (c) 400 °C annealed sample; (d) 500 °C annealed sample

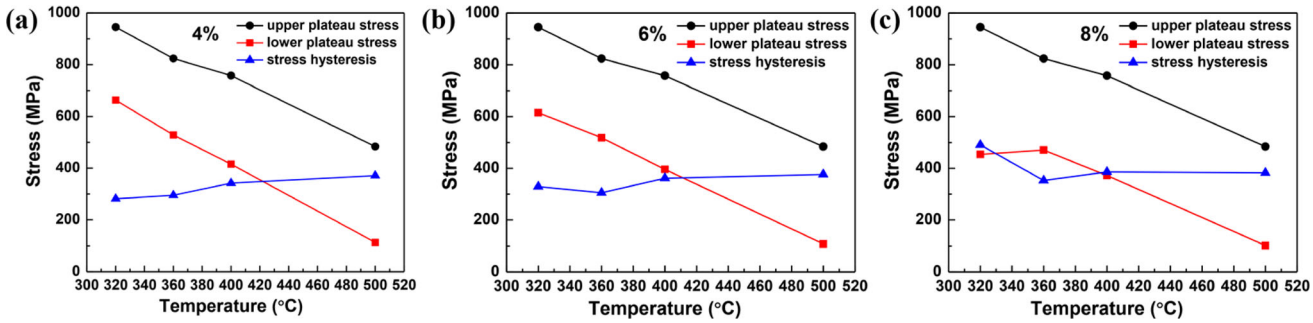

Fig. 3 Evolution of the upper and lower plateau stresses, and stress hysteresis with the annealing temperature of the 72% area-reduced NiTi wires during cyclic tensile deformation at different strains. (a) 4%; (b) 6%; (c) 8%

samples, the critical stresses of stress-induced martensitic transformation significantly decrease and unrecoverable plastic strains increase during cycling, indicating these samples have poor superelastic cycle stability. The reason for the poor superelastic cycle stability of these samples is that they undergo plastic deformation after undergoing Lüders-type martensitic transformation.

Figure 3 shows the evolution of the upper and lower plateau stresses, and stress hysteresis with the annealing temperature of the annealed NiTi wires with 72% area reduction, which obtained from the tensile curves in Fig. 2. It can be seen that the upper plateau stresses under all strains increase linearly with decreasing annealing temperature, which is attributed to the decrease of grain size (Ref 21, 22). Meanwhile, the lower plateau stresses under 4% and 6% strains also increase linearly with decreasing annealing temperature. However, the lower plateau stress under 8% strain of 320 °C annealed sample decrease compared to that of 360 °C annealed sample, causing the increase of stress hysteresis with decreasing annealing temperature in the temperature range of 320-360 °C. This behavior can be attributed to the occurrence of massive plastic deformation under 8% strain in 320 °C annealed sample.

In order to improve the superelastic cycle stability of the annealed NiTi wires with 72% area reduction, these samples are pre-deformed with strain of 9% to induce plastic deformation in advance, so that only elastic deformation and stress-induced martensitic transformation will occur in the subsequent deformation under a strain of less than 9%. Figure 4 shows the strain-controlled multi-step cyclic tensile curves (strains: 4%, 6% and 8%) of the 9% pre-deformed NiTi wires with 72% area

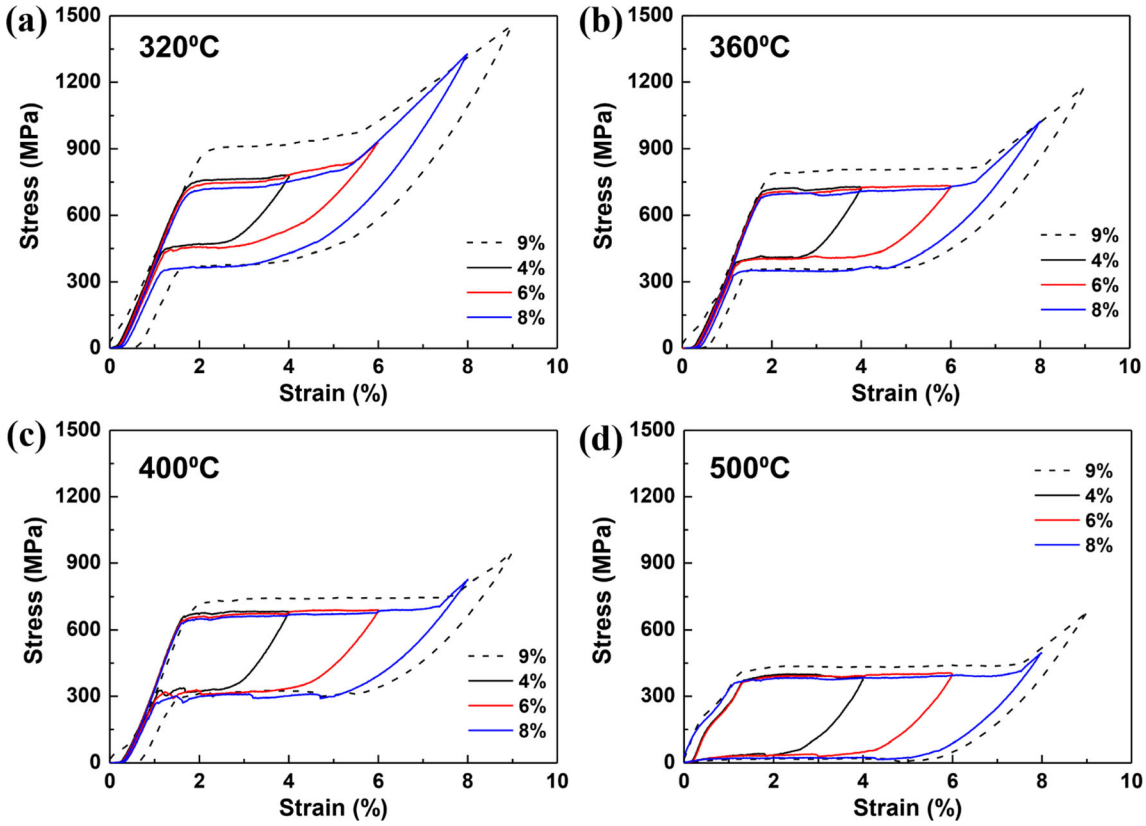

Fig. 4 Strain-controlled multi-step cyclic tensile curves (strains: 4%, 6% and 8%) of the 9% pre-deformed NiTi wires with 72% area reduction. The dotted lines are the tensile curve of 9% pre-deformation. (a) 320 °C annealed sample; (b) 360 °C annealed sample; (c) 400 °C annealed sample; (d) 500 °C annealed sample

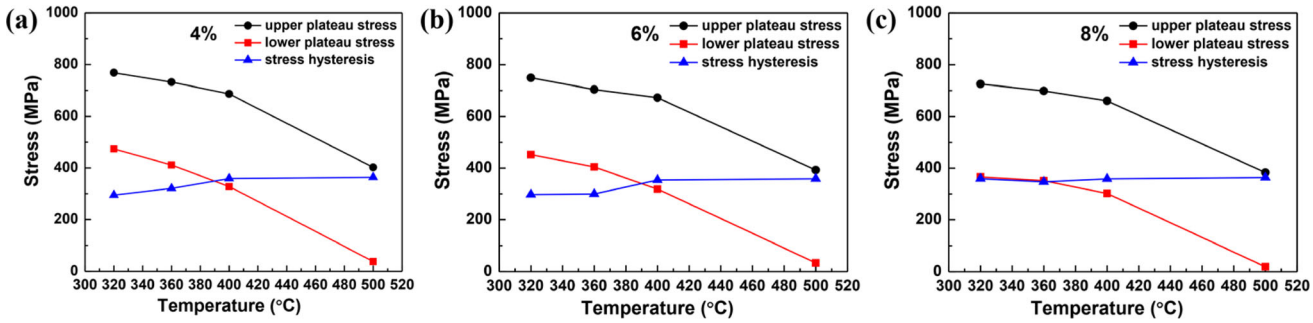

Fig. 5 Evolution of the upper and lower plateau stresses, and stress hysteresis with the annealing temperature of the pre-deformed NiTi wires with 72% area reduction during cyclic tensile deformation at different strains. (a) 4%; (b) 6%; (c) 8%

reduction. It can be seen that the critical stresses of stress-induced martensitic transformation remain basically unchanged during the subsequent cyclic deformation in all annealed NiTi wires after 9% pre-deformation, and there is almost no residual plastic strain in all samples after unloading. In brief, the superelastic stability of the pre-deformed NiTi wires is significantly improved compared to the above annealed samples. However, the critical stresses of martensitic transformation (upper plateau stresses) of all samples significantly decreased after pre-deformation. This is attributed to the plastic deformation that occurs in the pre-deformation, which leads to the generation of martensite nucleation points. These already existing martensite nucleation points reduce the stress required for martensite transformation. Meanwhile, it is noteworthy that pre-deformation has almost no effect on the lower plateau stresses in these samples.

Figure 5 shows the evolution of the upper and lower plateau stresses, and stress hysteresis with the annealing temperature of the pre-deformed NiTi wires with 72% area reduction, which obtained from the tensile curves in Fig. 4. It can be seen that the upper and lower plateau stresses under all strains increase linearly with decreasing annealing temperature. Meanwhile, the stress hysteresis decreases slightly with decreasing annealing temperature in the temperature range of 320-400 °C, and the stress hysteresis basically unchanged in the temperature range of 400-500 °C. In addition, it can be inferred from Fig. 4 and

5(c) that the occurrence of plastic deformation during pre-deformation can reduce the sensitivity of stress hysteresis to annealing temperature or grain size.

The above results (Figs. 2,3, 4, 5) show that plastic deformation has a significant effect on stress hysteresis of the NiTi wires with 72% area reduction. The true relationship between the stress-induced martensitic behavior of these samples and annealing temperature can be obtained from the 4% strain tensile curve. In order to better present the effect of pre-deformation on stress-induced martensitic transformation, Fig. 6 shows the evolution of the stress hysteresis during 4% tensile deformation and upper plateau strain with the annealing temperature of the NiTi wires with 72% area reduction. It can be seen from Fig. 6a that the stress hysteresis and upper plateau strain of the annealed samples both increase with increasing annealing temperature. As the annealing temperature increases from 320 to 500 °C, the stress hysteresis increases from about 280 MPa to about 370 MPa, and the upper plateau strain doubles from about 3 to 6%. In addition, it should be mentioned that when the annealing temperature is higher than 400 °C, the upper plateau strain remains essentially unchanged. For the 9% pre-deformed NiTi wires (Fig. 6b), both the stress hysteresis and upper plateau strain increase with increasing annealing temperature. Meanwhile, it can be seen that the stress hysteresis and upper plateau strain of the pre-deformed samples are slightly larger than those of the annealed samples at each annealing temperature. According to the results of Fig. 1 and Fig. 6, it is obvious that the stress hysteresis increases with increasing grain size, which shows a reverse effect to the results reported recently (Ref 7).

3.2 Sample with 35% area Reduction

Figure 7 shows the microstructure analysis of the NiTi wires with 35% area reduction. From the TEM bright-field image of the unannealed sample shown in Fig. 7(a), it is seen that the grains of the sample are elongated and appear in strip shapes. Meanwhile, the bright-field image reveals high-density dislocations in the sample. Figure 7(b) and (c) shows the corresponding SAED patterns of area A and B in the unannealed sample, respectively. It can be seen from the diffraction pattern that area A is B2 austenite grains and area B is B19' martensite grains. In the 320 °C annealed sample (as shown in Fig. 7d), the striped microstructure still exists, but the dislocations are greatly reduced compared to the unannealed sample. In the 400 °C annealed sample (as shown in Fig. 7e), most of the area recrystallizes to nanograins, and the average grain size is about 35 nm. In the 500 °C annealed sample (as shown in Fig. 7e), the recrystallized grains are larger, and the average grain size is about 80 nm.

Figure 8 shows the strain-controlled multi-step cyclic tensile curves (strains: 4%, 6% and 8%) of the annealed NiTi wires with 35% area reduction. It can be seen from Fig. 8(a) that when annealing at 320 °C, the sample exhibits homogeneous stress-induced martensitic transformation behavior. This behavior is attributed to the presence of high-density dislocations in 320 °C annealed sample (Fig. 7), and the dislocations act as the martensite nucleation points during tensile loading. Figure 8(b)–(d) shows that when annealing at higher temperatures (360, 400 and 500 °C), the samples experience Lüders-type stress-induced martensitic transformation. Combined with the TEM results in Fig. 7, it can be inferred that the grain morphology and dislocations in the NiTi wires have significant effect on their deformation behavior. In addition, compared to the annealed NiTi wires with 72% area reduction, the NiTi wires with 35% area reduction exhibit superior superelastic cycle stability. During 4% and 6% cyclic tensile deformation, the critical stress of stress-induced martensitic transformation of these samples is basically unchanged, and there is no residual plastic deformation after unloading. Their critical stress of martensitic transformation only slightly decreases during 8% cyclic deformation, and there is only about 0.3% residual plastic strain after unloading.

Figure 9 shows the evolution of the upper and lower plateau stresses, and stress hysteresis with the annealing temperature of the annealed NiTi wires with 35% area reduction, which obtained from the tensile curves in Fig. 8. It can be seen that the upper plateau stresses under all strains increase and then decrease with decreasing annealing temperature. Meanwhile, the lower plateau stresses under 4 and 6% strains increase with decreasing annealing temperature, but the lower plateau stress under 8% strain of decrease when the annealing temperature is below 360 °C. In addition, the stress hysteresis under all strains decrease with decreasing annealing temperature, but the rate of reduction decreases significantly with increasing deformation strain.

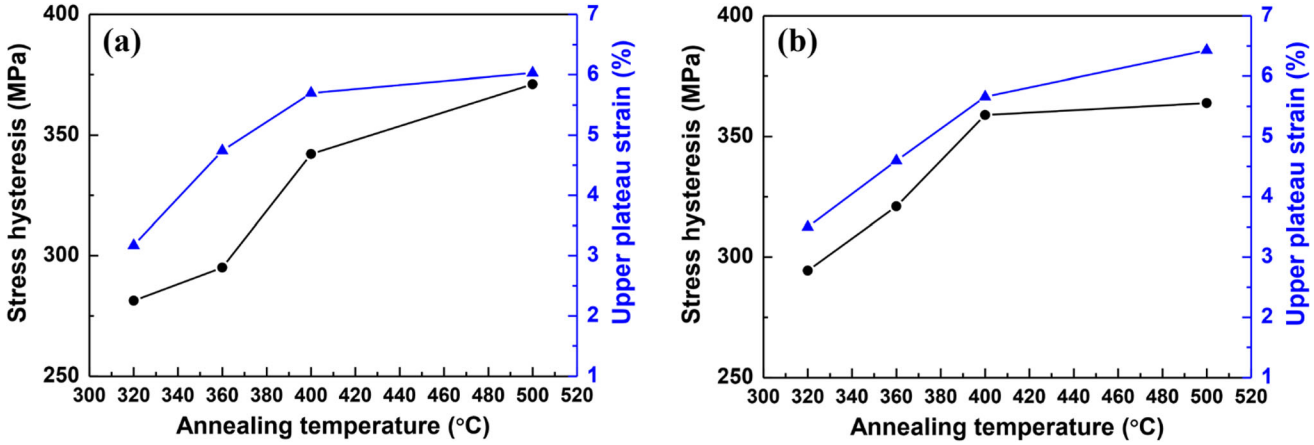

Fig. 6 Evolution of the stress hysteresis and upper plateau strain with the annealing temperature of the 72% area-reduced NiTi wires. (a) The annealed NiTi wires; (b) the 9% pre-deformed NiTi wires

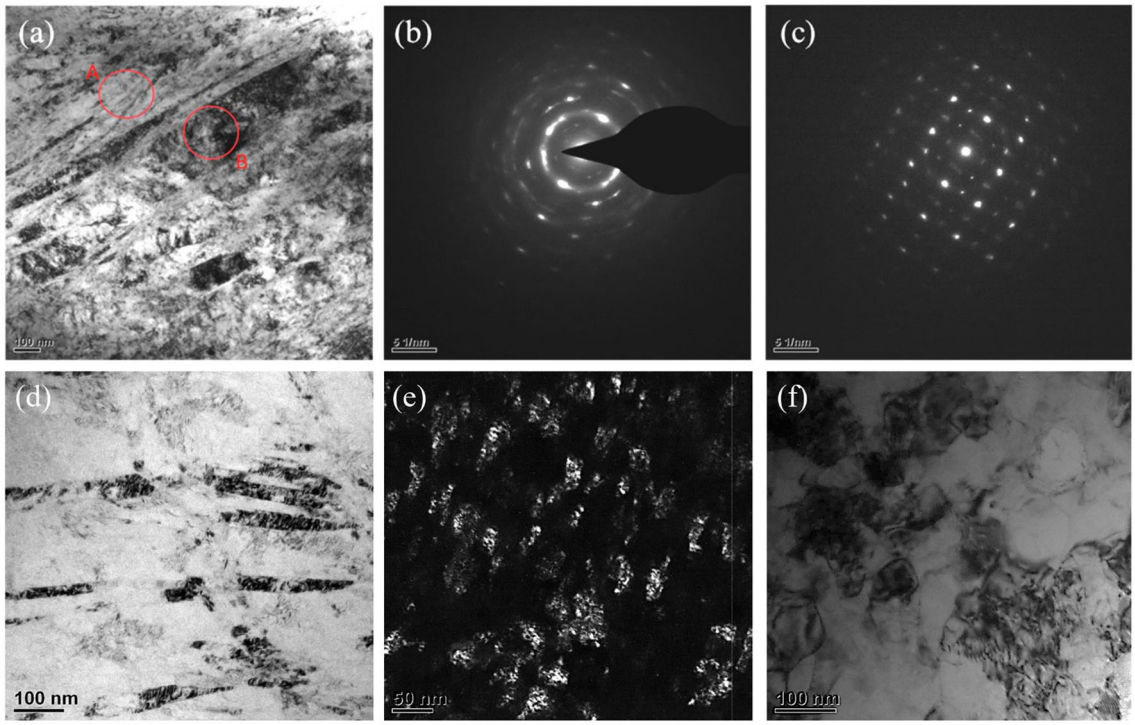

Fig. 7 Microstructure analysis of the NiTi wires with 35% area reduction. (a-c) The TEM bright-field image and corresponding SAED patterns of the unannealed sample; the TEM images of (d) the 320 °C annealed sample, (e) the 400 °C annealed sample and (d) the 500 °C annealed sample

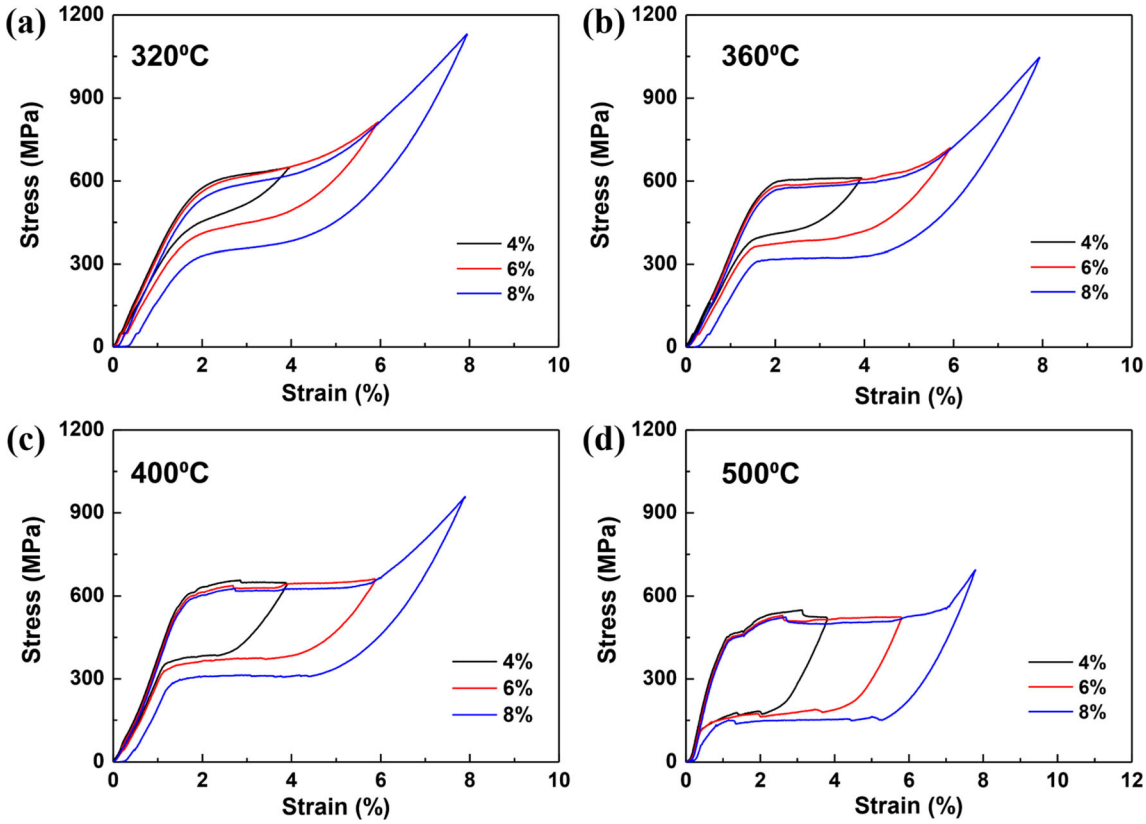

Fig. 8 Strain-controlled multi-step cyclic tensile curves (strains: 4%, 6% and 8%) of the annealed NiTi wires with 35% area reduction. (a) 320 °C annealed sample; (b) 360 °C annealed sample; (c) 400 °C annealed sample; (d) 500 °C annealed sample

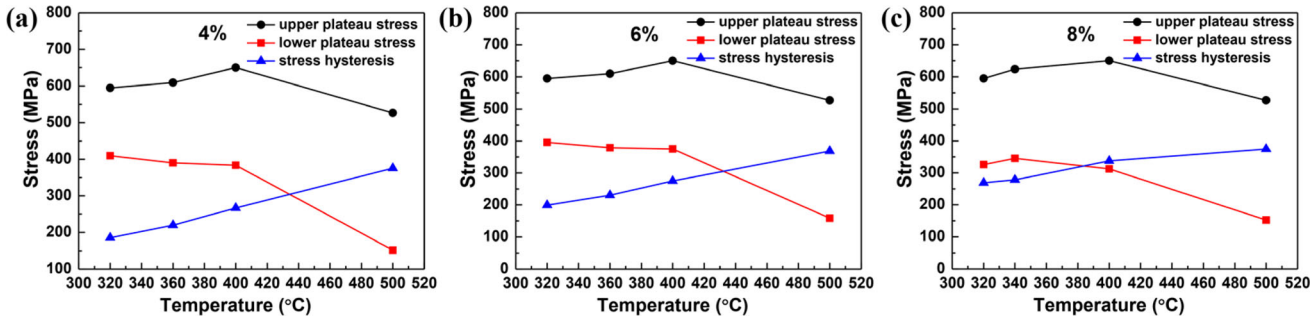

Fig. 9 Evolution of the upper and lower plateau stresses, and stress hysteresis with the annealing temperature of the 35% area-reduced NiTi wires during cyclic tensile deformation at different strains. (a) 4%; (b) 6%; (c) 8%

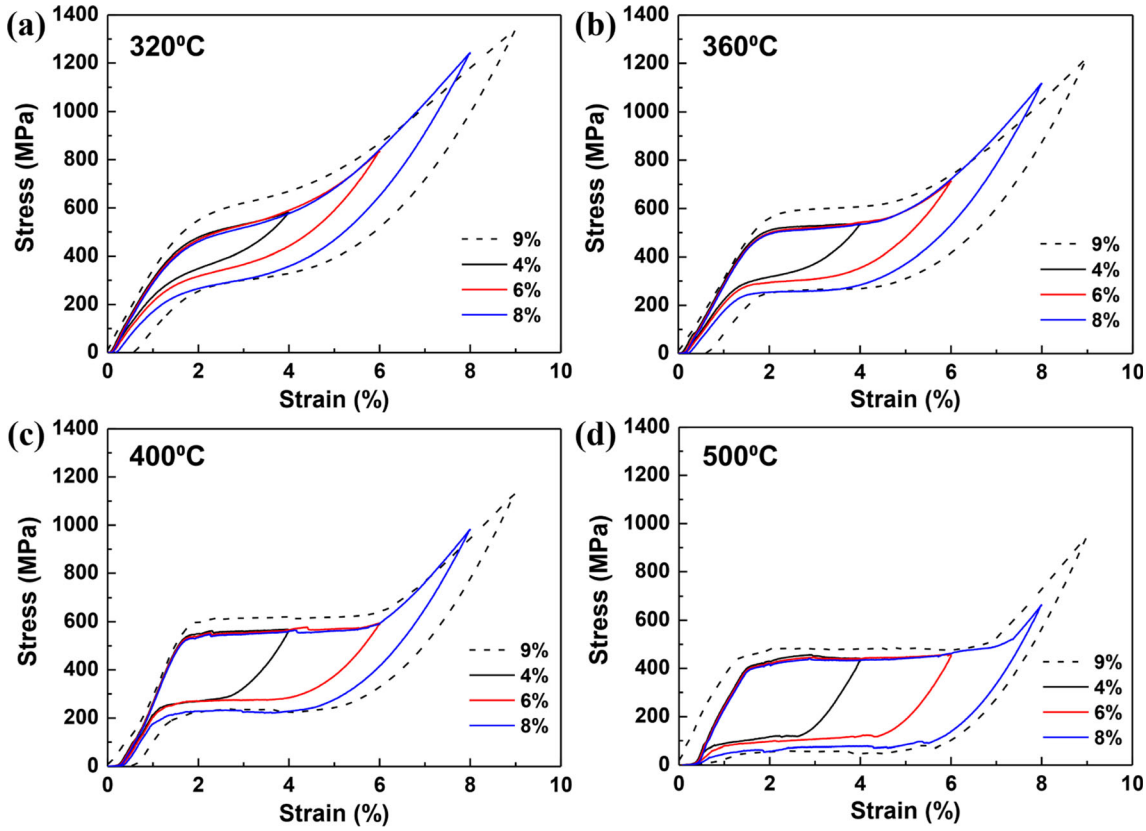

Fig. 10 Strain-controlled multi-step cyclic tensile curves (strains: 4%, 6% and 8%) of the 9% pre-deformed NiTi wires with 35% area reduction. The dotted lines are the tensile curve of 9% pre-deformation. (a) 320 °C annealed sample; (b) 360 °C annealed sample; (c) 400 °C annealed sample; (d) 500 °C annealed sample

Figure 10 shows the strain-controlled multi-step cyclic tensile curves (strains: 4%, 6% and 8%) of the 9% pre-deformed NiTi wires with 35% area reduction. It can be seen that the superelastic stability of these NiTi wires is further improved after pre-deformation compared to the above annealed samples. The critical stress of stress-induced martensitic transformation of these samples remain consistent during cyclic deformation and there is no residual plastic strain after 8% unloading. However, the critical stresses of martensitic transformation (upper plateau stresses) of all samples significantly decrease after pre-deformation. The disadvantage of pre-deformation is that it will cause a significant reduction in the critical stress of martensitic transformation. Therefore, when the deformation strain is less than 6%, pre-deformation of the NiTi wires with 35% area reduction is not recommended.

Figure 11 shows the evolution of the upper and lower plateau stresses, and stress hysteresis with the annealing temperature of the pre-deformed NiTi wires with 35% area reduction, which obtained from the tensile curves in Fig. 10. It can be seen that the upper plateau stresses under all strains increase and then decrease with decreasing annealing temperature, while the lower plateau stresses under all strains continuous increase. In addition, the stress hysteresis under all strains decrease with decreasing annealing temperature. Compared to the annealed NiTi wires with 35% area reduction (Fig. 9), the stress hysteresis of the pre-deformed samples is less affected by the deformation strain.

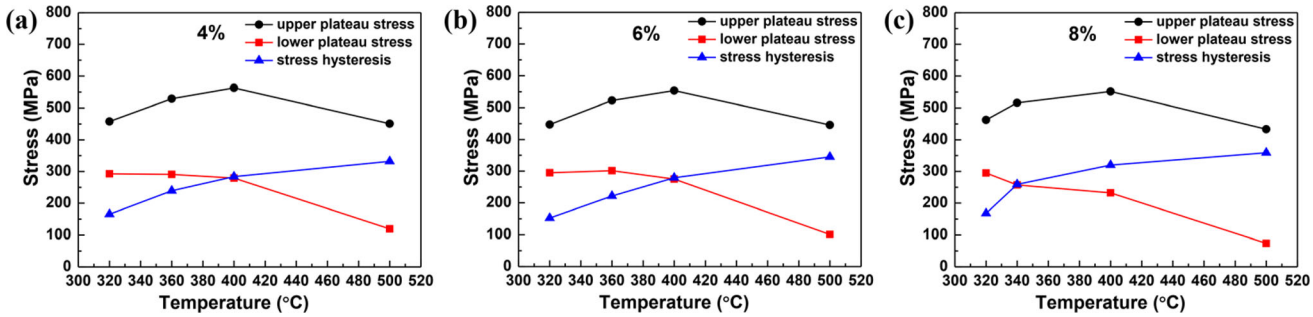

Fig. 11 Evolution of the upper and lower plateau stresses, and stress hysteresis with the annealing temperature of the pre-deformed NiTi wires with 35% area reduction during cyclic tensile deformation at different strains. (a) 4%; (b) 6%; (c) 8%

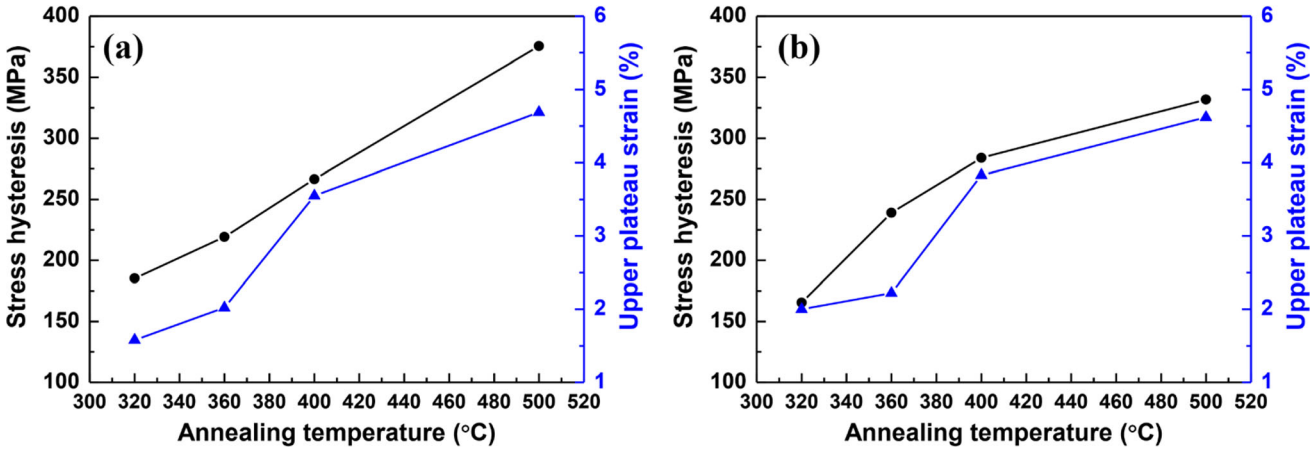

Fig. 12 Evolution of the stress hysteresis and upper plateau strain with the annealing temperature of the NiTi wires with 35% area reduction. (a) The annealed NiTi wires; (b) the 9% pre-deformed NiTi wires

Figure 12 shows the evolution of the stress hysteresis and upper plateau strain with the annealing temperature of the NiTi wires with 35% area reduction. It can be seen from Fig. 12(a) and (b) that the stress hysteresis and upper plateau strain of the annealed and the pre-deformed samples both increase with increasing annealing temperature. It should be mentioned that pre-deformation only slightly reduced the stress hysteresis of the 320 °C and 500 °C annealed NiTi wires, but it has little effect on that of the 320 °C and 500 °C annealed NiTi wires. In addition, pre-deformation also has little effect on the upper plateau strain all annealed samples.

4. Discussion

4.1 Critical Stress of Martensitic Transformation

It is seen in Fig. 2 that the critical stress of martensitic transformation of the annealed NiTi wires with 72% area reduction decreased with increasing annealing temperature. Combined with the TEM results in Fig. 1, it can be concluded that the martensitic transformation stress of this sample decreased with the increase of grain size. However, in the annealed NiTi wires with 35% area reduction, the martensitic transformation stress increased with increasing annealing temperature in the temperature range of 320-400 °C (Fig. 8). TEM results in Fig. 7 show that the dislocation density in the 400 °C annealed sample greatly reduced compared to the 320 °C annealed sample. Shi et al. reported that the martensitic phase nucleated at the stress concentration areas induced by the dislocations, and the number of nucleation sites increased with increasing dislocation density (Ref 7). Therefore, in the samples with 35% area reduction, the decreasing dislocation density increased the martensitic transformation stress in the temperature range of 320-400 °C. In addition, at the same annealing temperature, the 72% area-reduced sample exhibited a larger martensitic transformation stress compared to the 35% area-reduced sample, which is attributed to the smaller grain size and lower dislocation density of the 72% area-reduced sample.

Although the 72% area-reduced samples exhibited larger martensitic transformation stress compared to the 35% area-reduced samples, the martensitic transformation stresses of 72% area-reduced samples significantly decreased during cycling (Fig. 2). By contrast, the 35% area-reduced samples exhibited excellent superelastic cycle stability. When the 72% area-reduced samples had very few dislocations after annealing (Fig. 1), it can be inferred that there are few martensitic phase nucleation sites in these samples. After a loading and unloading, there were some martensitic nucleation points in these samples which were generated during the loading process, and these residual nucleation points can promote stress-induced martensitic transformation during the subsequent loading process, thereby reducing the martensitic transformation stress. In the 35% area-reduced samples, there were much nucleation sites induced by the dislocations, martensite was predominantly formed at these nucleation points during loading process, and

only a small number of new martensitic nucleation points were generated, so the martensitic transformation stresses in these samples were basically unchanged during the subsequent loading process.

After 9% pre-deformation, it is seen in Fig. 4 and 10 that the martensitic transformation stresses of 72 and 35% area-reduced samples both basically unchanged during cycling deformation, indicating the improvement of superelastic cycle stability by pre-deformation. This could be mainly attributed to the mass generation of martensitic nucleation points and the changes of the shape and orientation of grains during pre-deformation. It was reported that that the changes of the shape and orientation of the nanograins would facilitate the formation and growth of the martensite, and provided the mechanisms for grain shape accommodation on martensitic transforming (Ref 18). However, the pre-deformation significantly reduced the critical stress of martensitic transformation, so pre-deformation is not suitable for 35% area-reduced samples to improve superelastic stability.

4.2 Stress Hysteresis of Martensitic Transformation

In the annealed NiTi wires with 72% area reduction as shown in Fig. 3, the stress hysteresis of martensitic transformation of monotonically decreased with decreasing annealing temperature under 4% strain, but the stress hysteresis under 6 and 8% strains increased first and then decreased. These behaviors are different from the results of NiTi wires reported recently (Ref 7). In this previous work, the NiTi wires exhibited a two-stage yielding behavior at two Lüders-type stress plateaus, corresponding to the R-phase variant reorientation at the lower plateau and the stress-induced R $\rightarrow$ B19' transformation at the higher plateau (Ref 7, 15, 23). It had been reported that the twinning and interphase boundaries in R-martensite would increase the friction force for the movement of interphase R $\rightarrow$ B19' boundary, and thus increased the stress hysteresis (Ref 16). Therefore, we hypothesize that the increase in stress hysteresis with decreasing annealing temperature in the previously reported work is due to the increase in R-phase content and twinning interface. In our work, there is no R-phase variant reorientation plateau during loading (Fig. 2), and the decreased stress hysteresis can be attributed to the decrease of energy dissipation during stress-induced martensitic transformation with decreasing grain size (Ref 8). The increased stress hysteresis in 320 °C annealed samples under 6% and 8% strains is due to the occurrence of plastic deformation after Lüders-type martensitic transformation, which would increase the energy dissipation during loading.

It is seen in Fig. 9 that the stress hysteresis of martensitic transformation of the annealed NiTi wires with 35% area reduction decreased with decreasing annealing temperature. The annealing temperature effect on stress hysteresis is similar to the results acquired by A Ahadi and Shi et al (Ref 7, 8, 24). When the number of nucleation sites increased with increasing dislocation density, the interface between martensite and parent phases during nucleation and thus the interfacial energy would also increase (Ref 7). It has been reported that the stress hysteresis decreases with increasing interfacial energy (Ref 8, 24). Thus, the decrease in stress hysteresis in these samples is attributed to the increase of dislocation density with decreasing annealing temperature.

Pre-deformation exhibited a completely different effect on the stress hysteresis of the two types of samples (35% and 72% area reduction). For the NiTi wires with 72% area reduction, the stress hysteresis of pre-deformed samples is larger than that of the 320 °C, 360 °C and 400 °C annealed samples, as shown in Fig. 6. The increase of stress hysteresis is mainly attributed to the introduced dislocations by pre-deformation, which can be evidenced by the residual plastic strains in Fig. 4. These dislocations would increase the energy dissipation during subsequent deformation, and thus the stress hysteresis increased. Differently, pre-deformation has little effect on the stress hysteresis of the NiTi wires with 35% area reduction. This is attributed to the presence of dislocations in these samples prior to pre-deformation. The number of martensitic nucleation sites and thus the interface between martensite and parent phases during nucleation basically unchanged after pre-deformation.

5. Conclusions

The combined effect of annealing temperature and pre-deformation on the superelastic behaviors of NiTi shape memory alloy wires were investigated by testing two types of samples with 72% and 35% area reduction. The experimental evidence and the discussions present above allow the following main conclusions:

(1) The annealed NiTi wires with 72% area reduction exhibited larger martensitic transformation stress compared to the samples with 35% area reduction at the same annealing temperature. It is attributed to the smaller grain size and lower dislocation density of the 72% area-reduced sample.
(2) The annealed NiTi wires with 35% area reduction exhibited superior superelastic cycle stability compared to the samples with 72% area reduction. It is attributed to the higher dislocation density and thus the presence of much more martensitic nucleation points in the 35% area-reduced samples.
(3) The stress hysteresis of martensitic transformation decreased with decreasing annealing temperature for both types of NiTi wires with 72% and 35% area reduction. In addition, the occurrence of plastic deformation during loading would increase the stress hysteresis of both samples.
(4) Pre-deformation enhanced the superelastic cycle stability of both NiTi wires; however, it also led to notable decrease in the critical stress of martensitic transformation.
(5) Pre-deformation increased the stress hysteresis of the NiTi wires with 72% area reduction, but reduced their sensitivity of stress hysteresis to annealing temperature. In contrast, pre-deformation has little effect on the stress hysteresis of the NiTi wires with 35% area reduction.

Acknowledgment

This work was supported by the National Natural Science Foundation of China (No. 52201214, 52071142 and 52001121), the Natural Science Foundation of Beijing (No. 2232065), Natural Science Foundation of Hebei Province (No. E2024502028, E2022502011 and E2022502004), Science and Technology Plan-

ning Project of Baoding Municipality (No.2372P011) and the Fundamental Research Funds for the Central Universities, China (No. 2023MS132 and 2024MS131).

Conflict of interest

No potential conflict of interest was reported by the author(s).

References

1. J. Mohd Jani, M. Leary, A. Subic, and M.A. Gibson, A Review of Shape Memory Alloy Research, Applications and Opportunities, *Mater. Des.*, 2014, **56**, p 1078–1113.
2. L.G. Machado and M.A. Savi, Medical Applications of Shape Memory Alloys, *Brazilian J. Med. Biol. Res.*, 2003, **36**, p 683–691.
3. J. Van Humbeeck, Non-Medical Applications of Shape Memory Alloys, *Mater. Sci. Eng. A*, 1999, **273**, p 134–148.
4. K. Otsuka and X. Ren, Physical Metallurgy of Ti-Ni-Based Shape Memory Alloys, *Prog. Mater. Sci.*, 2005, **50**, p 511–678.
5. K. Tsuchiya, Mechanisms and Properties of Shape Memory Effect and Superelasticity in Alloys and Other Materials: A Practical Guide, *Shape Mem. Superelastic Alloy.*, 2011 https://doi.org/10.1533/9780857092625.1.3
6. R. Delville, B. Malard, J. Pilch, P. Sittner, and D. Schryvers, Transmission Electron Microscopy Investigation of Dislocation Slip during Superelastic Cycling of Ni-Ti Wires, *Int. J. Plast.*, 2011, **27**(2), p 282–297. https://doi.org/10.1016/j.ijplas.2010.05.005
7. X.B. Shi, F.M. Guo, J.S. Zhang, H.L. Ding, and L.S. Cui, Grain Size Effect on Stress Hysteresis of Nanocrystalline NiTi Alloys, *J. Alloys Compd.*, 2016, **688**, p 62–68. https://doi.org/10.1016/j.jallcom.2016.07.168
8. Q. Ahadi Palcheghloo, Aslan; Sun, Stress Hysteresis and Temperature Dependence of Phase Transition Stress in Nanostructured NiTi—Effects of Grain Size, *Appl. Phys. Lett.*, 2013, **103**, p 021902.
9. Z. Zhao, J. Lin, Y. Xiao, and J. Min, Effects of Grain Size and Dislocation Density on Thermally-Induced Martensitic Transformation of Nanocrystalline NiTi Alloys, *J. Alloys Compd.*, 2024, **978**, p 173490. https://doi.org/10.1016/j.jallcom.2024.173490
10. P. Sedmák, P. Šittner, J. Pilch, and C. Curfs, Instability of Cyclic Superelastic Deformation of NiTi Investigated by Synchrotron X-Ray Diffraction, *Acta Mater.*, 2015, **94**, p 257–270.
11. X. Kong, Y. Yang, S. Guo, R. Li, B. Feng, D. Jiang, M. Li, C. Chen, L. Cui, and S. Hao, Grain-Size Gradient NiTi Ribbons with Multiple-Step Shape Transition Prepared by Melt-Spinning, *J. Mater. Sci. Technol.*, 2021, **71**, p 163–168. https://doi.org/10.1016/j.jmst.2020.07.034
12. X. Kong, H. Ding, J. Zhang, Q. Liu, J. Wang, J. Zhou, F. Qi, P. Wang, S. Hao, and Y. Ren, Study on Phase Transformation, Internal Stress and Texture Evolution of Cold Drawn Nb Nanowire-NiTi Composite Wires upon Annealing, *Intermetallics*, 2023, **163**, p 108066. https://doi.org/10.1016/j.intermet.2023.108066
13. Z. Deng, K. Huang, H. Yin, and Q. Sun, Temperature-Dependent Mechanical Properties and Elastocaloric Effects of Multiphase Nanocrystalline NiTi Alloys, *J. Alloys Compd.*, 2023, **938**, p 168547. https://doi.org/10.1016/j.jallcom.2022.168547
14. T. Wang, F. Guo, Y. Li, and J. Ye, The Superelastic Stability of Nanocrystalline Ni-51 At% Ti Shape Memory Alloy, *J. Mater. Eng. Perform.*, 2024, **33**(9), p 4633–4639. https://doi.org/10.1007/s11665-023-08251-3
15. X. Shi, L. Cui, D. Jiang, C. Yu, F. Guo, M. Yu, Y. Ren, and Y. Liu, Grain Size Effect on the R-Phase Transformation of Nanocrystalline NiTi Shape Memory Alloys, *J. Mater. Sci.*, 2014, **49**(13), p 4643–4647.
16. E.E. Timofeeva, N.Y. Surikov, A.I. Tagiltsev, A.S. Eftifeeva, E.Y. Panchenko, and Y.I. Chumlyakov, The Orientation Dependence of Thermal and Stress Hysteresis at R-B19' Martensitic Transformation in Aged Ni50·6Ti49.4 Single Crystals, *J. Alloys Compd.*, 2020, **817**, p 1–7.
17. K. Xu, J. Luo, C. Li, Y. Shen, C. Li, X. Ma, and M. Li, Mechanisms of Stress-Induced Martensitic Transformation and Transformation-Induced Plasticity in NiTi Shape Memory Alloy Related to Superelastic Stability, *Scr. Mater.*, 2022, **217**, p 114775. https://doi.org/10.1016/j.scriptamat.2022.114775
18. X.B. Shi, Z.C. Hu, X.W. Hu, J.S. Zhang, and L.S. Cui, Effect of Plastic Deformation on Stress-Induced Martensitic Transformation of Nanocrystalline NiTi Alloy, *Mater Charact*, 2016, **2017**(128), p 184–188.
19. Y. Cui, A. Zhao, H. Yan, and X. Zeng, The Effect of Pre-Deformation Loading on the Cyclic Hysteresis Behavior of Nanocrystalline NiTi Alloy: A Molecular Dynamic Study, *Vacuum*, 2023, **218**, p 112613. https://doi.org/10.1016/j.vacuum.2023.112613
20. G. Tan, Y. Liu, P. Sittner, and M. Saunders, Lüders-like Deformation Associated with Stress-Induced Martensitic Transformation in NiTi, *Scr. Mater.*, 2004, **50**(2), p 193–198.
21. W. Tang, Q. Shen, X. Yao, W. Li, J. Jiang, Z. Ba, Y. Li, and X. Shi, Effect of Grain Size on the Microstructure and Mechanical Anisotropy of Stress-Induced Martensitic NiTi Alloys, *Mater. Sci. Eng. A*, 2022, **849**, p 143497. https://doi.org/10.1016/j.msea.2022.143497
22. T. Waitz, V. Kazykhanov, and H.P. Karnthaler, Martensitic Phase Transformations in Nanocrystalline NiTi Studied by TEM, *Acta Mater.*, 2004, **52**(1), p 137–147.
23. B. Feng, X. Kong, S. Hao, Y. Liu, Y. Yang, H. Yang, F. Guo, D. Jiang, T. Wang, Y. Ren, and L. Cui, In-Situ Synchrotron High Energy X-Ray Diffraction Study of Micro-Mechanical Behaviour of R Phase Reorientation in Nanocrystalline NiTi Alloy, *Acta Mater.*, 2020, **194**, p 565–576. https://doi.org/10.1016/j.actamat.2020.05.004
24. A. Ahadi and Q. Sun, Stress-Induced Nanoscale Phase Transition in Superelastic NiTi by in Situ X-Ray Diffraction, *Acta Mater.*, 2015, **90**, p 272–281. https://doi.org/10.1016/j.actamat.2015.02.024